



A hybrid solar/biomass active indirect kiln dryer for timber in the Democratic Republic of Congo

Silvia Ferrari, Ignazia Cuccui, Paolo Cerutti & Ottaviano Allegretti

To cite this article: Silvia Ferrari, Ignazia Cuccui, Paolo Cerutti & Ottaviano Allegretti (2024) A hybrid solar/biomass active indirect kiln dryer for timber in the Democratic Republic of Congo, International Journal of Ambient Energy, 45:1, 2367109, DOI: [10.1080/01430750.2024.2367109](https://doi.org/10.1080/01430750.2024.2367109)

To link to this article: <https://doi.org/10.1080/01430750.2024.2367109>



© 2024 The Author(s). Published by Informa UK Limited, trading as Taylor & Francis Group.



Published online: 09 Jul 2024.



Submit your article to this journal [↗](#)



Article views: 308




View related articles [↗](#)



View Crossmark data [↗](#)

A hybrid solar/biomass active indirect kiln dryer for timber in the Democratic Republic of Congo

Silvia Ferrari ^a, Ignazia Cuccui ^b, Paolo Cerutti ^a and Ottaviano Allegretti ^b

^aCIFOR-ICRAF Center for International Forestry Research and World Agroforestry, Kisangani, DRC; ^bCNR IBE, National Research Council Istituto per la BioEconomia, San Michele all'Adige, Italy

ABSTRACT

This paper presents a small-scale pilot project in the Democratic Republic of Congo of a hybrid kiln dryer for sawn timber powered by solar and biomass energy. The chamber's thermal insulation comprised layers of vetiver grass, wood and clay, 100% biodegradable. Sun collectors and a supplementary furnace-burning biomass from the nearby sawmill provided the heating energy, while photovoltaic panels supplied electric energy for ventilation and electric devices. The climate was controlled through actuators operated by an electronic system for industrial kiln dryers. Despite relatively high production costs, primarily due to the photovoltaic system, the kiln allowed for good use of local labour and materials. Preliminary tests indicated an improved drying potential of the kiln compared external conditions with a consequent lower drying time and final MC. Data emphasised the influence of thermal energy in the drying rate: the extra power given by the furnace increased the drying rate from 0.4 to 1.4% day⁻¹. The cost of energy (\$/kWh) was calculated as 0.009 for the furnace, 0.05 for the solar collector and 0.14 for the photovoltaic. The conversion efficiency of solar collector resulted to be 48% against 14% of photovoltaic.

ARTICLE HISTORY

Received 9 March 2024
Accepted 6 June 2024

KEYWORDS

Solar timber dryer; tropical hardwoods; wood seasoning; wood drying; sustainable technology; developing countries

Nomenclature

c	Specific heat capacity of water [kWh kg ⁻¹ C° ⁻¹]
DIF	Diffuse horizontal irradiation (kW m ⁻²)
DT	Drying test
EMC	Equilibrium moisture content (%)
EMC _{ext}	Equilibrium moisture content of air outside the dryer (%)
EMC _{int}	Equilibrium moisture content of air inside the dryer (average left–right side) (%)
EMC _{set}	Set equilibrium moisture content of air inside the kiln (%)
FR	Referred to furnace
G	Drying potential (MC/EMC)
GHI	Global Horizontal Irradiation (kW m ⁻²)
L	Latent heat of vaporisation [kWh kg ⁻¹]
MC _{av}	Average Moisture Content of the wood (average of n.8 probes) (%)
MC _f	Final Moisture Content of the wood (%)
MC _i	Initial Moisture Content of the wood (%)
M _w	Mass of water stored in the tank (kg)
PREC	Precipitation of rain (mm)
PV	Referred to photovoltaic plant
q	Flow rate of water in the circuit (kg h ⁻³)
Q _D	Thermal energy dissipated during the passage of water in the circuit section (kWh)
Q _{FR}	Thermal energy produced by the furnace (kWh)
Q _{KD}	Thermal energy absorbed by the water–air heat exchanger in the kiln dryer (kWh)

Q _{PV}	Electric energy produced by photovoltaic (kWh)
Q _{SC}	Thermal energy produced by the solar collector (kWh)
RH	Relative humidity (%)
SC	Referred to solar collector
T _{ext}	Temperature of air outdoor (°C)
T _{int}	Temperature of air inside the dryer (average left–right side) (°C)
T _{set}	Set temperature of air in the kiln
T _{Win}	Temperature of water entering the heat exchanger (°C)
T _{Wout}	Temperature of water exiting the heat exchanger (°C)
T _{Wt}	Temperature of water in the storage tank (°C)
V	Volume of wood of the stack (m ³)
W	Weight of the water evaporated (kg)
ρ ₀	Oven-dry density of wood (kg m ⁻³)

1. Introduction

Nearly 64% of the Democratic Republic of Congo (DRC) is covered by tropical moist forests, accounting for about 150 million hectares (ha). This represents two-thirds of the total forest cover of the Congo Basin (Guizol et al. 2022). Forest harvesting occurs through an industrial, large-scale, export-oriented concessionary model, and a small-scale, individual, artisanal model, primarily serving the domestic market. The latter produces 10 times more sawn timber than the former, exceeding 1 million cubic metres (m³) annually (Lescuyer et al. 2014). Commonly traded wood species include *Pericopsis elata* (afroformosia), *Milicia*

excelsa (iroko), *Gilbertiodendron dewevrei* (limbali), *Afzelia bipindensis* (doussié), and various species of the *Entandrophragma* genus (sipo, sapelli, tiama and kosipo). Some of these species, such as afrormosia and doussié, are listed in annex II of the Convention on International Trade in Endangered Species of Wild Fauna and Flora (CITES 2023) signifying their endangered status and the need for regulated and authorised trade. Despite the assigned role of forest stewardship to artisanal loggers within the DRC legal framework, a significant portion of production occurs outside this framework.

Compared to the industrial model, the small-scale artisanal value chain and in particular timber harvesting and processing do not occur on the base of solid technical knowledge and appropriate equipment. The habit of using obsolete and basic equipment as axe and chainsaw for felling trees and wood processing to produce sawn timber results in substantial waste of time and of precious raw material (Duhesme et al. 2022). Yet artisanal timber production usually neglects drying process leading to poor-quality final products.

The common practice of using wood with excessively high Moisture Content (MC), causes shrinkage, warping and cracks in the final product; biological attacks decay wood with a MC higher of 18–20%. A final MC ranging from 15% (for decking carpentry and exterior use) to 10% (for flooring, joinery and interior use) is recommended for potential exports (Joly and More-Chevalier 1980).

Timber drying occurs through natural seasoning and/or artificial drying. Natural seasoning is typically the best practice for the pre-drying stage, enabling a transition from MC higher than 40% (green wood) to around 20% (Joly and More-Chevalier 1980). Artificial drying, although demanding energy, trained personnel and initial investments, provides better control of quality and productivity and allows a lower final MC. The success of artificial drying depends on the knowledge of the kiln operator and kiln performance. Over the past 50 years, scientific and technological developments have transformed timber drying from an empirical activity into a codified industrial process, which controls drying parameters to achieve constant productivity and quality (Bond and Espinoza 2016; Elustondo et al. 2023). Different drying quality grading standards regulate the national and international trade of timber in most countries (European Standard 14298: 2018 Saw timber – Assessment of drying quality 2018; EDG (European Drying Group) – Recommendation 1994). Key quality parameters include final MC (average and variability), deformations, cracks, collapse and internal stress. Drying schedules, optimising the drying rate/quality ratio, have been assessed for most wood species on each continent, and consider various thicknesses (Boone et al. 1988).

Solar dryers are a relatively cheaper and sustainable alternative to conventional steam-heated kilns, particularly for small operations. They hold great potential in developing countries, especially in remote locations with limited access to conventional energy. Solar drying falls into two main categories: direct (open-air sun drying) and indirect (convective solar drying). Depending on the process (direct or indirect), solar dryers may be classified as passive (heated directly from the sun with or without natural air circulation) or active (where hot drying air circulates using a ventilator, known as forced convection) (Mathew and Venugopal 2021; Ndukwu, Bennamoun, and Abam 2018).

Options for solar energy production include thermal or photovoltaic collectors. The former is easily adaptable for drying and has a flexible design. The latter entails higher costs and complexity, demanding investment when electricity is required for forced air circulation and kiln control (Ndukwu, Bennamoun, and Abam 2018).

Efficiency of thermal energy storage is a major concern with respect to maintaining acceptable drying conditions within the kiln, mitigating day/night differences, and avoiding mould, even if positive effects of oscillating drying are reported in some conditions (Bond and Espinoza 2016). The experience of solar drying in African countries, with experimental and modelling results, is documented in Ndukwu, Bennamoun, and Abam (2018). Udomkun et al. (2020) review adoption of solar drying technology for agricultural products in Asia and sub-Saharan African countries, including DRC. Numerical and experimental works published in the last decade for solar drying of wood are summarised and analysed by Lamrani et al. (2022). In the study of Bekkioui et al. (2023), a forced convection solar dryer for thuya wood drying was investigated with computer simulation. The mathematical model proposed was used to study and compare the wood moisture content, drying air temperature and wood temperature variations with very satisfactory model-predicted results.

Solar dryers are often small-capacity devices, relatively simple in design. Most are used for drying crops and food for family use or for some small-scale industrial production (Chauhan and Rathod 2020; Ndukwu, Bennamoun, and Abam 2018). In Central Africa, within the tropical rainforest range, the climate is warm and humid for most of the year. The daily Global Horizontal Irradiation (GHI) is around $5 \text{ kWh m}^{-2} \text{ day}^{-1}$ (Solargis 2023) among the lowest on the continent. For this area, a few documented cases refer to solar dryers for vegetables in Cameroon (Berinyuy, Tangka, and Weka Fotso 2012) and cassava chips in DRC (Udomkun et al. 2020).

The work here presented was integrated into a broader intervention in the area called FORETS, a project by the Center for International Forestry Research (CIFOR) and financed by the European Union (<https://www2.cifor.org/forets/>).

Because of the significative role of the artisanal timber value chain in reducing forest degradation, one of the main objectives of FORETS project was to improve this value chain by creating a new sustainable model of production in collaboration with local communities. Ultimately, it led to production of semi-finished sawn timber for various end uses through a relatively economical and easily replicable model.

The present work contributes to this main objective of the project by focusing on timber drying with the specific aim of developing an innovative drying system adapted to the artisanal context and characterised by positive economic, social and environmental benefits.

The case study took place in a village in the Tshopo Province of DRC. The authors designed, built and tested a prototype solar kiln dryer for timber harvested by local artisanal loggers.

The innovation apported by this work can be resumed at three levels: (i) almost all the materials used for realising the kiln have local origin with a preference for sustainable ones. The chamber and most of the part of the plant (excluded the electronic control) is plastic-free and made with 100%

Table 1. Average monthly climatic conditions in Yanonge (Solargis).

Month	GHI	DIF	T	RH	EMC	PREC
	kWh m ⁻²	kWh m ⁻²	°C	%	%	mm
Jan	165.1	91.8	25.8	82	16.7	77.0
Feb	154.6	83.6	26.4	80	15.9	97.4
Mar	170.6	87.7	26.1	85	17.8	159.2
Apr	156.1	75.7	25.6	88	19.2	165.5
May	154.7	74	25.4	89	19.6	144.5
Jun	136.9	79.3	25.1	88	19.2	111.2
Jul	135	86.6	24.8	88	19.2	118.8
Aug	144.5	85.6	24.6	89	19.7	160.4
Sep	153.3	79.8	24.6	89	19.7	191.6
Oct	156.8	75.8	24.7	90	20.1	202.3
Nov	144.8	75.6	24.6	90	20.2	191.4
Dec	152.1	86.6	25.1	88	19.2	117.7
sum	1824.5	982.1				1737
average	152.0	81.8	25.2	87.2	18.8	144.8

biodegradable materials; (ii) the kiln has been entirely built by a local and trained team using both traditional and modern knowledges. This social aspect is essential in such a remote context because the participation of natives in developing this new technology can facilitate its adoption and replication in the future; (iii) the specific technology adopted has been chosen on the base of the study of the literature review on solar drying in sub-Saharan regions – which is, by the way, much more focused in vegetables than in timber – together with the analysis of what was effectively possible to realise *in situ*.

2. Materials and methods

The case study was conducted in the village of Yanonge (WGS84: N 0.592 E 24.718) in the Tshopo Province of DR Congo. In this location, a small sawmill with a potential annual production capacity of up to 300 m³ of semi-finished products had already been implemented and launched as part of the main project led by CIFOR.

Yanonge overlooks the left bank of the Congo River, the major transport route for goods, people and materials via pirogues and boats. The nearest city with materials and specialised craftspeople (welders, electricians, etc.) is Kisangani, approximately half a day away. Logistics are generally complicated, and the market for materials and products can fluctuate quickly. Common materials like sheet glass or aluminium can be hard to find or very expensive, prompting the need to adapt the plant's design based on the availability of materials.

Table 1 reports the average monthly climate at this location. The daily GHI ranges from 3.4 to 5.8 kWh m⁻² day⁻¹ with an average annual value of 5.0 kWh m⁻² day⁻¹ (Figure 1). Average monthly relative humidity (RH) is always above 80% and often close to saturation. In these conditions, natural seasoning of green planks takes a long time and the Equilibrium Moisture Content (EMC) of seasoned wood never drops below 18–20%.

According to the psychrometric chart, sensible heating of the air from 25° to 40°C in the confined space of a kiln dryer would drop RH from 80% to 20%. As such, total drying time (from 40% to a final MC = 15–18% of 50 mm thick sawn boards) takes about 20 days (Simo-Tagne and Bennamoun 2018). Based on this scenario, a 4 m³ kiln capacity was deemed sufficient for the target production. This was set at 20–30 m³/year of timber dried to a final MC of 15–18% for the internal market and 12% or

less for export markets. The first step of natural seasoning from green to pre-dried (MC = 20–30%) is planned for an area with a canopy annexed to the sawmill, which can stock up to 60 m³ of ventilated stacks sheltered from rain and direct solar radiation.

The budget for the prototype was set at around \$50,000. It assumes that, for a higher amount, different commercial plants become a competitive option. Whenever possible, priority was given to expenses for locally sourced labour and materials.

Preliminary studies and experiences directed us toward an active indirect dryer for consistent and uniform production. The active indirect kiln dryer, resembling a traditional convective kiln dryer, is equipped with heat exchangers, fans and vents controlled by a system to maintain RH and T within the target values of the adopted drying schedule. This setup involves a forced circulation of air facilitated by electrical fans to convect heat and vapour between the wood and the surrounding air in the kiln and to vent humid air outside. Thermal energy from an external source is stored and transported to the drying chamber using water or other fluids moved by a pump in a closed circuit.

2.1. Climatic control and data acquisition system

The architecture of the climatic control system is composed of (a) probes measuring the drying parameters; (b) actuators electrically operated; and (c) the digital control unit that detects the drying parameters and acts on the actuators according to the scheduled logic to keep T and RH of the air in the kiln within set values (Figure 2).

2.1.1. Probes

- 7 T pt100 sensors with a typical accuracy of ±0.15°C at 0°C were placed in different parts of the plant measuring water and air temperature.
- Two T-RH probes were installed inside the kiln (T-RH_{int}) and one T-RH probe was installed outside the kiln (T-RH_{ext}). RH probes were capacitive sensors with an accuracy of ±1.5% in the RH range of 0–99%. RH value, coupled with T value, was converted by the control in the corresponding EMC value with the *Hailwood Horrobin Equation* (Babiak 2007). For simplicity, EMC of air as a function of such RH and T is always reported in the results instead of RH.
- 6 Wood MC metres resistive sensors type, each one composed of two metallic electrodes screwed into the wood plank. The accuracy is about ±2–5% in the MC range of 5–45%. The relation between MC and the mass of water (W) contained in the wood with volume (V) and oven-dry density (ρ_0) is given by:

$$W = MC\rho_0V [\text{Kg}] \quad (1)$$

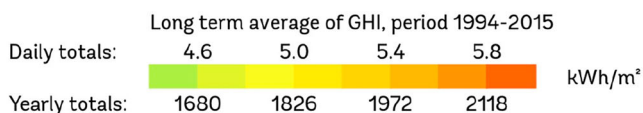
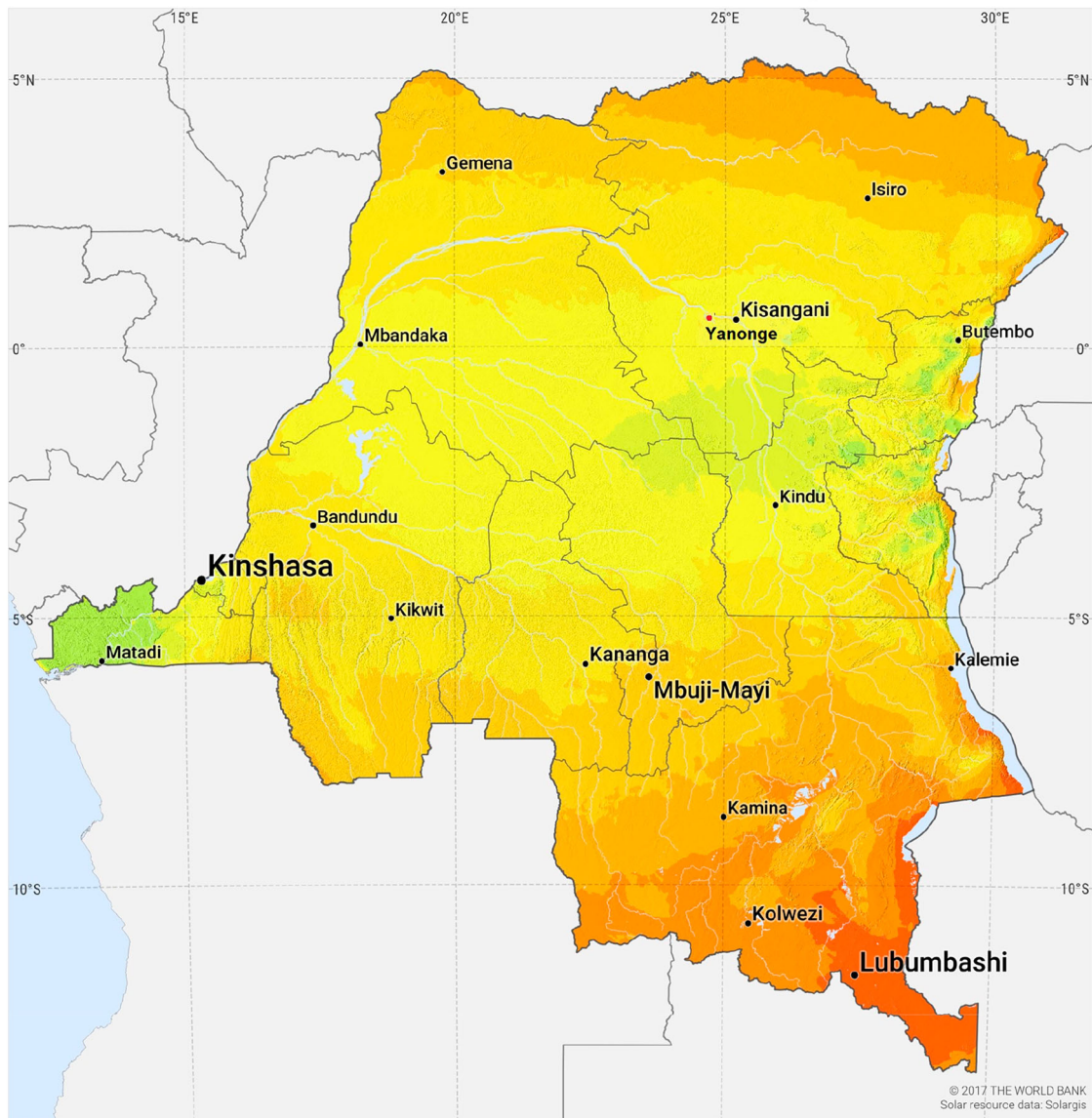
2.1.2. Aerothermal actuators

The following equipment was installed in the chamber as actuators activated by the control:

- n. 2 × aluminium axial fans Ø 300 mm, powered by 2 × 0.75 kW – 220 V motors. Speed 1400 RPM, airflow: 3.080 m³/h; static pressure 15.7 mm H₂O; Dynamic pressure 1.19 H₂O; declared air velocity 4.35 m/s.
- n. 2 × Ø mm 150 vents with proportional flaps.

SOLAR RESOURCE MAP

GLOBAL HORIZONTAL IRRADIATION DEMOCRATIC REPUBLIC OF THE CONGO



This map is published by the World Bank Group, funded by ESMAP, and prepared by Solargis. For more information and terms of use, please visit <http://globalsolaratlas.info>.

Figure 1. GHI in RDC 2020 The World Bank, source: Global Solar Atlas 2.0, solar resource data: Solargis.

- n. 1 $2 \times 1.5 \times 0.7$ m heat exchanger in aluminium finned tubes.
- n. 1 water pump: flow rate = 2400 kg/h, power absorption = 93 W.

2.1.3. Control unit

A *dTouch* control produced by *Logica H&S* (Logica H&S SRL Electronics for wood processing 2023) equipped with the probes described was installed. It is WEB-connected, allowing full

supervision, programming and data download from any remote PC. Data recorded at a given sampling rate are the signal from the probes and the status of the actuators (ON/OFF; %).

The control allows keeping T and RH of air in the kiln at set values, activating the actuators (flaps, valves, etc). When T_{int} is lower than the set point temperature (T_{set}) and the T_{wt} , the control switches on the water pump to increase temperature. When EMC_{int} is higher than EMC_{set} , the control opens the vents to allow air exchange and to decrease EMC_{int} .

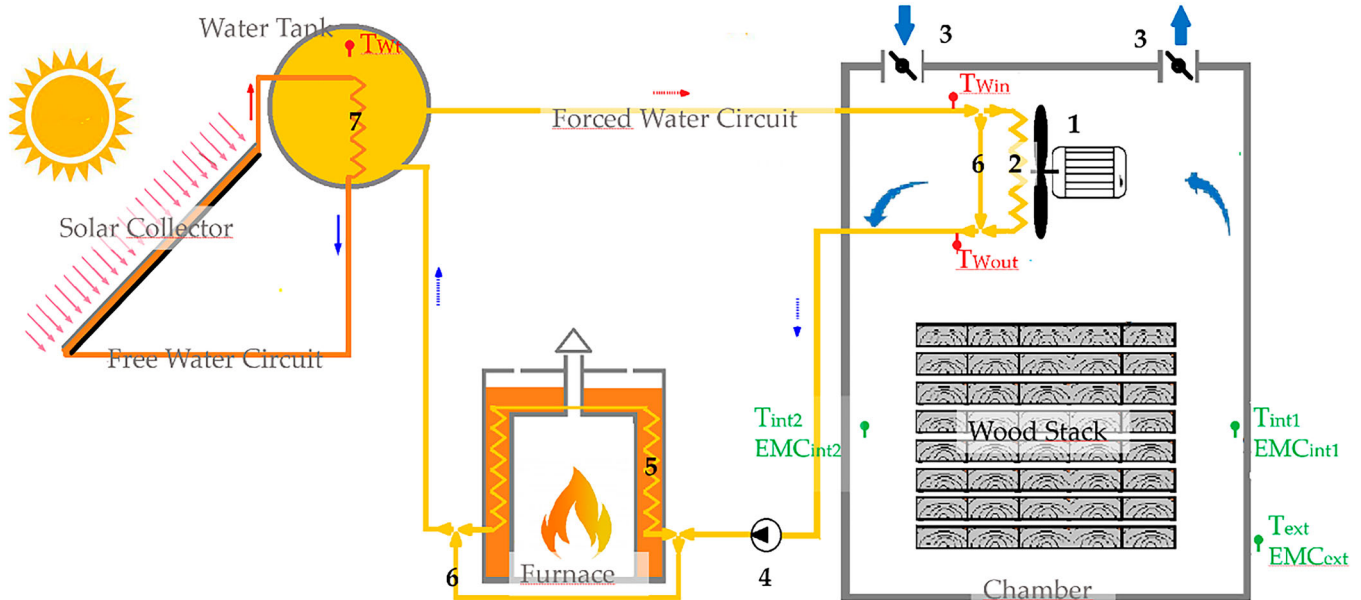


Figure 2. Layout of the thermo-aerodynamic system (aleatory scale and disposition of elements). Note: (1) fan and motor, 2) water–air heat exchanger; (3) vents; (4) water pump; (5) water–water heat exchanger of furnace; (6) by-pass; (7) water–water heat exchanger of Solar Collector. Green captions: T and RH air probes. Red caption: T water probes.

The EMC_{set} and T_{set} are dependent on MC, the wood species, and the lumber thickness (Allegretti et al. 2009). They are defined by the drying schedule, unless the kiln operator overrides the manual set point value. The drying schedule can be generated by the control that contains a database of more than 400 wood species. The control system can absorb up to 40 W of power.

2.2. Energy system

The energy need for conventional wood drying reportedly (Lamrani et al. 2022) ranges from 600 to 1000 kWh m⁻³ of wood or nearly 2 kWh kg⁻¹ of extracted water. Electrical energy for ventilation represents 5–10%, thermal energy is 90–95%. Accordingly, the energy system for the kiln dryer has been sized to provide energy in the range of 80–200 kWh day⁻¹ with 4–20 kWh day⁻¹ of electrical energy.

For electricity, we installed 19.8 m² of photovoltaic panels (PV) with a total nominal installed power capacity of 4.15 kW-peak and an expected daily production of around 14–15 kWh day⁻¹ (0.7 kWh day⁻¹ m⁻²). The electric energy storage system was composed of 12,200 Ah 12-V batteries (total energy storage: 28.8 kWh). Given a global electrical power absorption of about 1.65 kW (fans + control + pump), in operative conditions and sunny days, the system is designed to provide enough energy to run the fans about 40% and the control 100% of the time.

The thermal energy system was limited in this first developing step to a small (3.4 m²) commercial flat solar thermic collector natural circulation type, with a tilt of 15° oriented to the west and an auxiliary homemade furnace for biomass (Figure 3). This hybrid configuration was chosen to try to balance the budget constraints with the need of a flexible energy production that can cover night-time deficits and consumption peaks. At the same time, it allowed to collect data on system efficiency and operative limits that look ahead to a possible expansion of the thermal system.



Figure 3. Back side of the completed kiln with the small technical room (hosting the control and the electric panel), the furnace, the flat solar thermic collector and the water tank. Note: The seasoning area of the sawmill can be seen beyond the kiln.

The solar collector and furnace are connected in parallel to a forced water circuit (moved by the water pump) that collects, stores and transports thermal energy as depicted in Figure 2. Collector inclination was the minimum prescribed by the producer for efficient natural circulation. It was higher than the 3° indicated by the literature (Bracamonte et al. 2015) as an optimum tilt for maximum energy generation.

The furnace, locally designed and assembled, was made from a metallic cylinder. It has a double wall where a copper coil water–water heat exchange takes place immersed in the water reservoir (confined between the double wall of the furnace) heated by the fire burning in the inner part of the furnace (4 of Figure 2). The water reservoir of the furnace is an open system to prevent overpressure of the water flowing in the close circuit.

Thermal energy is stored in a 300 kg insulated water tank. The thermal energy produced by the sun collectors is transferred to

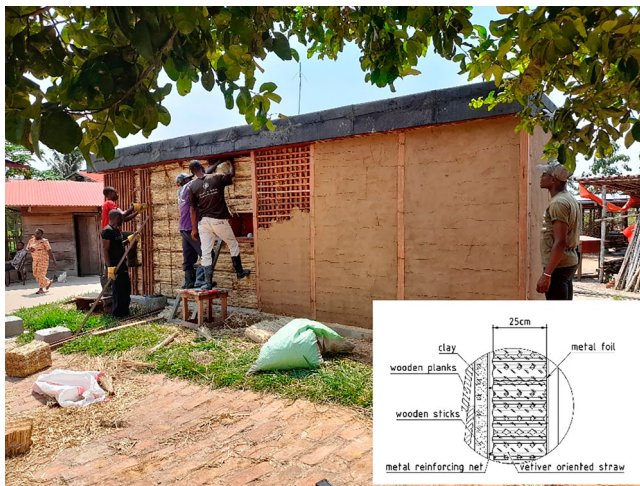


Figure 4. Back wall of the chamber during construction of insulating layers. Note: Bottom right: section of the walls from the exterior (left) to the interior (right).

the water in the tank by a water-water exchanger (4 of Figure 2) while the hot water produced by the furnace is directly transported to the water in the tank by the water pump. The pump moves water to the water-air heat exchanger inside the kiln (2 of Figure 2) directly activated by the thermostatic function of the control according to the air temperature in the kiln.

2.3. The chamber

The structural bearing frame of the chamber ($6.7 \times 1.6 \times 2.2$ m) was made of iron square pipe (section 2×4 cm) with solder connections on concrete foundation (5×8 m). The chamber can host a wooden stack $5 \times 1 \times 1.5$ m corresponding to a capacity of about 4 m^3 of wood. The volume surplus of the chamber was designed for a sufficient air circulation around the stack. A door on the long side of the box allows charging and discharging the kiln. An internal metal layer provided vapour tightness (needed for optimal humidity control in the kiln). The metal layer was soldered along the edges and protected by a layer of epoxy resin and a rubber gasket along the door's edge.

The insulating layer of the chamber was provided by vetiver blocks with fibers perpendicular to the heat flux. The thickness was 25 cm for the walls and roof and 8 cm for the door. The blocks were handmade from fresh vetiver straw, harvested, and air dried for about two weeks and then compressed and tied with twine. The final block's density was $140 \pm 20 \text{ kg/m}^3$. The insulation composite was eventually completed (Figure 4) with one layer of clay and one layer of wood planks. The vetiver layer of the door was reduced to 8 cm of thickness.

Vetiver grass (*Chrysopogon zizanioides* Roberty), used as insulation material, is a perennial grass native to India, South and Southeast Asia but widely cultivated in tropical regions for its interesting properties (Gnansounou, Alves, and Raman 2017). It grows rapidly up to 1.5 m and adapts to harsh conditions and limited water with minimal maintenance. Unlike other grasses that develop horizontal roots, vetiver roots grow downwards up to 3 m; they quickly colonise the land and are often used to avoid soil erosion and enhance soil quality. Other studies have reported various experiences of applications of vetiver as

a building material. It has been used as ash to form a mortar (sewers, foundations, marine infrastructures) (Nimityongskul, Panichnava, and Hengsadeeukul 2003). It has reinforced bundles for a clay matrix (Hengsadeeukul and Nimityongskul 2004) and also been used simply as straw to make roofs. Vetiver is water-proof, repels insects and has high durability (Gnansounou, Alves, and Raman 2017). Cascone, Rapisarda, and Cascone (2019) provide a better understanding of straw bale systems, especially their insulating properties (thermal and acoustic) and durability.

2.4. Drying tests

The paper reports results about the two first drying tests labelled DT1 (started on November 21/2022, lasted 39 days) and DT2 (started on April 19/2023, lasted 18 days), both carried out during the rainy season.

In DT1 the furnace was switched on (FR-ON state) only during the last stage (days from 27 to 30). Consequently, the solar thermal panels only supplied energy during the longest part of the test (FR-OFF period). The ventilation was rationed following an ON/OFF constant intermittency of two hours. In DT2 the furnace was always ON during the day hour and OFF during night hours (from 24:00 to 6:00). Ventilation was always OFF during such night hours and kept intermittently during the day.

The kiln was loaded with 3.8 m^3 of 20 mm thick sawn boards with an initial MC in the range 20–50% of sapelli and oboto in DT1 and kosipo in DT2. Main drying properties of such species found in literature are reported in Table 2.

According to the recommended drying schedule T_{set} rises from 40° to 50° C and the EMC_{set} decreases from 13% to 7% as a function of MC.

2.5. Energy balance

The total energy balance (Q_{TOT}) of the process is given by:

$$Q_{PV} + Q_{KD} + Q_D = Q_E + Q_{FR} + Q_{SC} \text{ [kWh]} \quad (2)$$

where the left part of the equation is the energy consumed and the right one is the energy produced.

The electric energy consumed by the electrical actuators (Q_{PV}) can be easily calculated knowing their power absorption and ON/OFF state at each sampling step. It corresponds to the energy produced by photovoltaic (Q_E) as directly displayed by inverter.

The thermal energy consumed is calculated from the temperature difference of the water measured at each sampling step in two points in water circuit, and from q_w , the flow rate of the water pump. When the pump is ON, the water circulates in a loop from the tank to the air-water heat exchanger to the furnace and then back to the tank (see Figure 2). The highest water temperature is in the tank (T_{Wt}), collecting energy produced by the solar collector and/or by the furnace. The lowest temperature occurs just before water reaches the furnace (T_{Wout}) when energy has been consumed. The total thermal power consumed is therefore given by:

$$E_D + E_{KD} = c q (T_{Wout} - T_{Wt}) \text{ [kW]} \quad (3)$$

E_D is the energy dissipated during the passage of water in the circuit section from T_{Wt} to T_{Win} .

Table 2. Wood species tested and their main technological and drying properties as found in literature.

	Sapelli	Oboto	Kosipo
	<i>Entandrophragma cylindricum</i> Sprague	<i>Mammea Africana</i> G. Don	<i>Entandrophragma Candollei</i>
Density [kg m ³]	690	750	700
Drying behaviour	Variable drying properties with slow drying and marked tendency to warp	From moderately difficult to difficult with risk of checks	Risk of checks, warping and collapses
Recommended drying schedule	2D4 (Boone et al. 1988), A type (Pratt 1974)	'2' (TROPIX 7 The main technological characteristics of 245 tropical wood species 2017)	2D4 (Boone et al. 1988), A type (Pratt 1974)

E_{KD} is the thermal energy transferred inside the kiln by the water–air heat exchanger consumed for evaporation and thermal dispersion through the chamber's walls.

The effective thermal power of the sun collector (E_{SC}) delivered to the water tank was determined from the time derivative of temperature of the water in the tank (dT_{wt}/dt) recorded at two consecutive sampling steps:

$$E_{SC} = c M_w (dT_{wt}/dt) \text{ [kW]} \quad (4)$$

E_{SC} was measured from data collected at a logging rate of one reading per minute at different hours of the day and in different days when the state of the furnace and the water pump was OFF. During such OFF states, energy accumulated in the water tank is produced by the solar collector only and it is not consumed for drying (in the air–water exchanger).

The thermal energy production of the furnace (Q_{FR}) was determined indirectly from Equation (1) where Q_{KD} , Q_D and Q_{SC} are known (Equations (3) and (4)) (Figure 3).

The energy (Q_{KD} ; Q_D) consumed from the beginning to the end of the process at each sampling step $t = [t_0, t_1 \dots t_n] E = [E_0, E_1 \dots E_n]$ is finally calculated with:

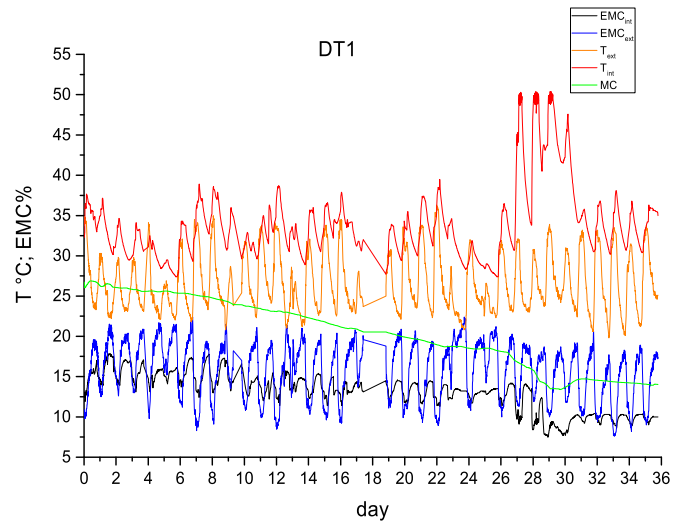
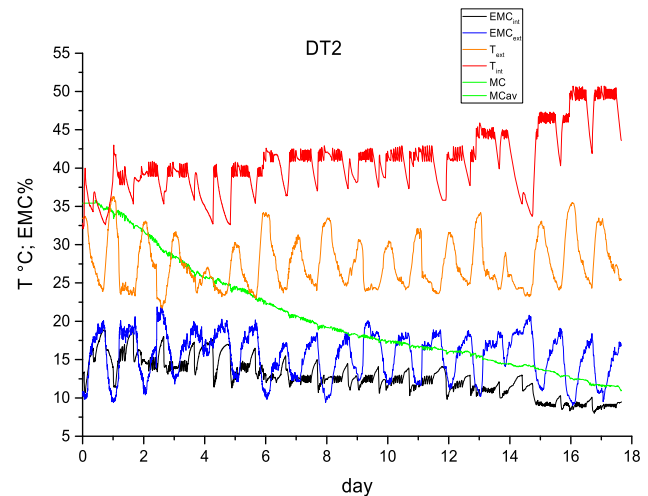
$$Q = \sum_{i=0}^n t_i E_i = t * E \text{ [kWh]} \quad (5)$$

3. Results

3.1. Process parameters

The time series of the main process parameters of DT1 and DT2 are reported in Figures 5 and 6 and condensed in Table 3. Statistics of external and internal climatic conditions of DT1 (FN-OFF period only) and DT2 are compared in Figure 7. The most relevant difference is a higher T_{int} in DT2 than DT1, while EMC_{int} is similar but always lower than EMC_{ext} , above all during the daily hours (Figure 8).

The drying gradient G (or drying potential), expressed as MC/EMC , is one of the main factors influencing the drying rate. In Figure 9, measured G of the drying tests (MC/EMC_{int}) is plotted against average MC and it is compared with G calculated with data of the external climatic conditions (MC/EMC_{ext}) and with G profile of the standard drying schedule adopted. It can be observed that G in DT1 and DT2 overlaps and it is lower than the commercial drying schedule but higher than G in exterior conditions meaning a general improvement in the drying potential compared to external conditions. The figure suggests also the convenience of a pre-drying stage from green to about 25% when $G_{int} \geq G_{ext}$. Finally, since G profiles of DT1 and DT2 are about the same, the observed difference in drying rates (-0.4% and -1.4% per day) is attributed solely to the temperature of

**Figure 5.** Evolution of the main drying parameters during the drying tests DT1.**Figure 6.** Evolution of the main drying parameters during the drying tests DT2.

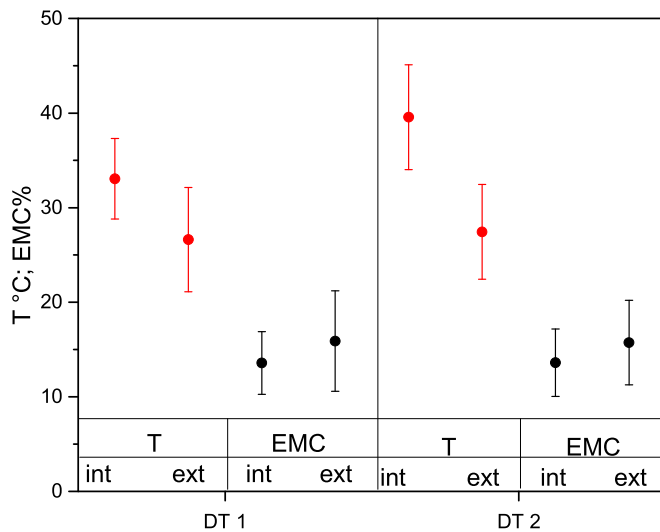
the air, directly depending on the power energy availability and influencing the vapour and heat transfer coefficients.

3.2. Energy

The daily power production curve of solar collectors (E_{SC}) and photovoltaic panels (E_{PV}) measured during the tests as described in section 2.5 are compared in Figure 10 with the expected GHI of the period (Solargis 2023). Based on those curves, average daily production was, respectively, 2.42 (SC), 0.72 (PV) and 5.0 (GHI) kWh m⁻² day⁻¹. The conversion efficiency in relation to the GHI

Table 3. Drying tests: Main process parameters.

			DT1	DT2	DT1 tot	DT2 tot	Literature
Average initial MC	MC _i	%	28	28	28	35	
Average final MC	MC _f	%	18	18	14	11	
Average T of air	T _{int}	°C	32.8	38.9	34.0	39.6	
Average EMC of air	EMC _{int}	%	14.3	13.9	13.3	13.6	
Water removed	W	kg	253	260	327	645	
Total time		days	26	7	36	18	
Av. drying rate		% day ⁻¹	0.4	1.4	0.4	1.4	
	E _{av}	kW	1.0	4.7	2.0	5.3	
Total energy consumed	Q _{TOT}	kWh	625	813	1719	2227	
Energy contribution of single source on the total	Q _{PV} /Q _{TOT}	%	63	11	29	12	
	Q _{FR} /Q _{TOT}	%	0	83	54	82	
	Q _{SC} /Q _{TOT}	%	37	6	17	6	
	Q _{TOT} /W	kWh kg ⁻¹	2.5	3.1	5.3	3.5	1.9 (Simo-Tagne and Bennamoun 2018)
	Q _{TOT} /V	kWh m ⁻³	156	203	430	557	500–1200 (Simo-Tagne and Bennamoun 2018)
Drying efficiency	WL/Q _{TOT}	%	25.4	20.1	11.9	18.2	20.5% (López-Sosa et al. 2019)

**Figure 7.** Interval plot of internal/external T and EMC (average and 95% of the confidence interval).

was 48% for SC and 14% for PV. The average power of the furnace (E_{FR}) resulted from 4 kW to 12 kW with a biomass consumption of about 2.5 kg/kWh.

The trend of energy vs MC consumed during the process, divided into its individual components, is shown in Figure 11 where one can observe (especially in DT2) that the trend of total energy consumption ($Q_{TOT} = Q_D + Q_{KD} + Q_{PV}$) is almost constant when MC is above 25% and it increases exponentially when MC drops below the saturation point. This expected result is due to the surplus of energy needed to evaporate the bound water, which increases (from about 0.6 kW kg⁻¹ for free water up to 1 kW kg⁻¹) as the MC decrease.

A comparison of the process efficiency between the kiln operating in its two main thermal power configurations, (i.e. the FR-OFF period of DT1 and FR ON period of DT2) can be performed by observing data related to a homogeneous MC range (18% < MC < 28%) as reported in the first two columns of Table 3 (alongside the total value at the conclusion of the drying processes in the last two columns). Within this MC range the

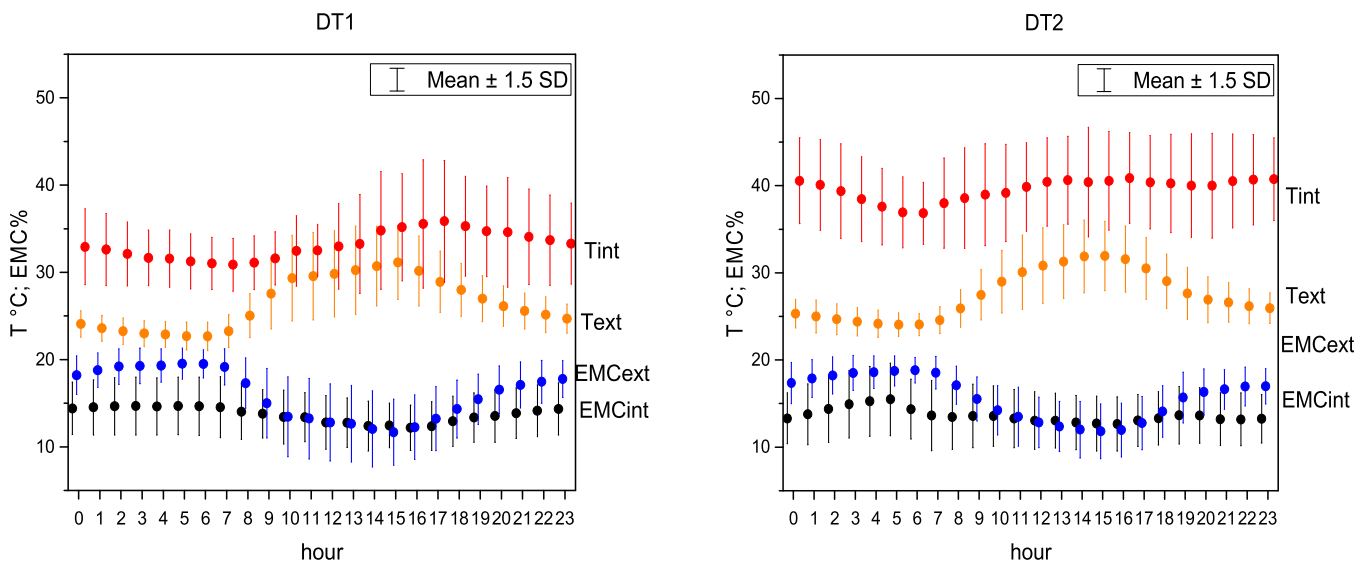
**Figure 8.** Interval plot of average internal/external T and EMC vs. hour of the day of DT1 (FR-OFF period only) (a) and DT2 (average and 95% of the confidence interval) (b).

Table 4. List of the cost for the prototype rounded to the nearest hundred (*: materials bought locally).

Component description		Costs (USD)			Man Hours
		Materials	Labour	TOT	
Box	Concrete foundation	*3000	1600	4600	336
	Bearing structure	*7700	4400	12100	960
	Vetiver thermic insulation	*2300	2600	3900	4203
Energy	Solar thermic system and hydraulic circuit	*3000	600	3600	168
	Furnace	*1900	800	2700	192
	Photovoltaic system	17400	400	17800	128
Actuators	Control	2300		2300	
	Fan	300		300	
	Motors	500		500	
	Pump	300		300	
	Vents	800		800	
	Total	39500	10500	50000	5987

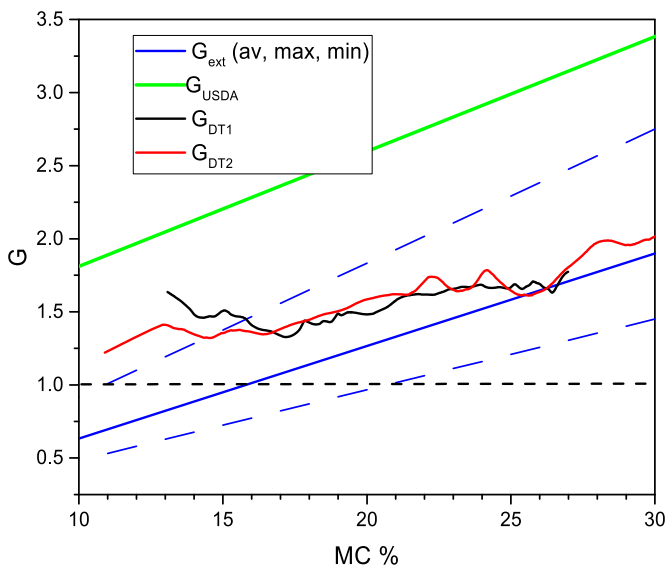
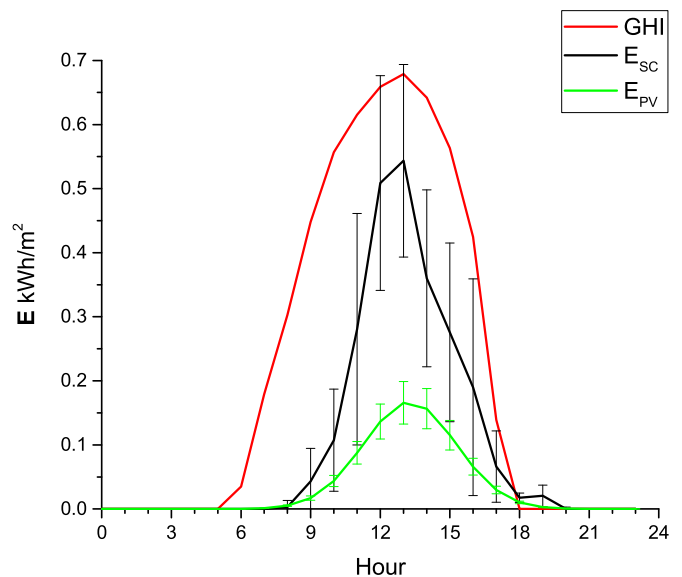
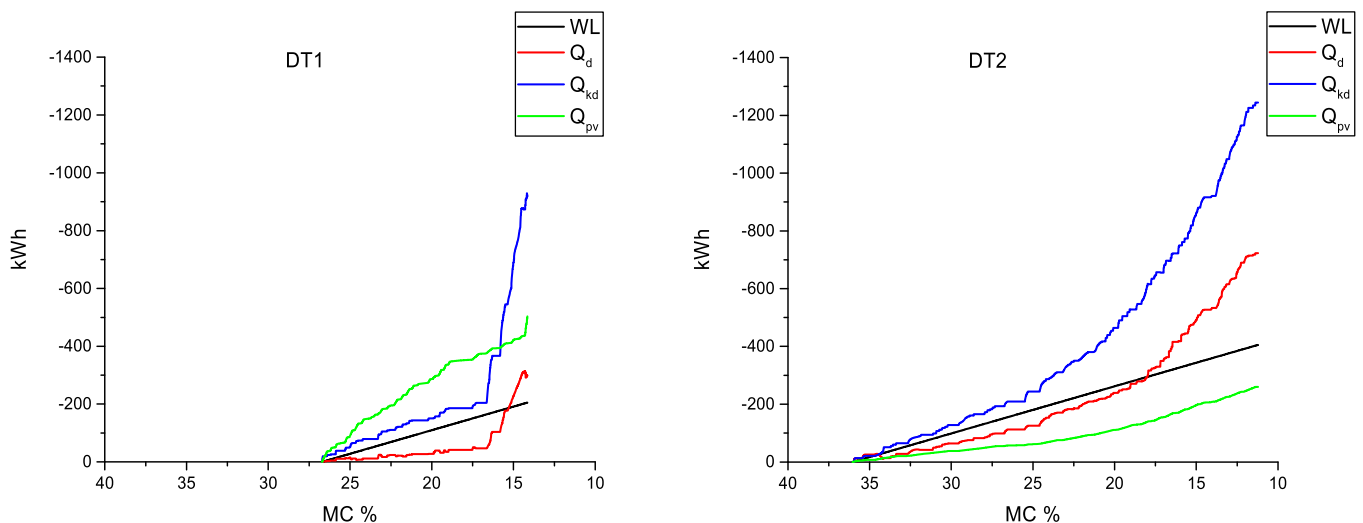
**Figure 9.** Drying potential (G) plotted against average MC. Note: Black and red lines: G as measured in DT1 and DT2. Blue lines: G (average maximum and minimum) calculated at external climatic conditions. Green line: G according to standard drying schedule 'USDA 2D4'. G lower than 1 (dot line) indicates a condition when the wood tends to adsorb MC from the surrounding environment.**Figure 10.** Daily average power curves of flat solar collectors (E_{sc}) photovoltaic panels (E_{pv}) and GHI (Global Horizontal Irradiation).**Figure 11.** Evolution of the different components of energy during DT1(a) and DT2(b). Q_d and Q_{kd} are the components of the thermal energy supplied by the solar collector and/or by the furnace, as described in the nomenclature table.



Figure 12. View of the inner part of the kiln with the stack at the end of the drying process.

average power supplied was 1 and 4.7 kW, respectively, with a significant different input of electric energy which contributed respectively for 63% and 11% on the total energy input, in part transformed into heating through the Joule effect.

As a result of such differences, the drying rate increased from 0.4 to 1.4%/day, and the drying efficiency decreased (because of a higher thermal dispersion) from 25.4% to 20.1%.

The stack of dried lumbers at the end of DT2 is reported in Figure 12 also showing a view of the inner part of the kiln. Drying quality assessed by visual grading resulted good in terms of absence of cracks and warping.

3.3. Costs

Table 4 reports the costs incurred for the prototype. Based on the data above, assuming a life expectancy of 25 years and productivity of 30 m³/year, depreciation of the investment would be USD 67 per m³ of dried wood. Sapelli sawn timber is traded in local and European markets at about USD 700 and USD 1,500, respectively. Thus, depreciation can add 4–10% to the cost of raw materials.

Construction labour on the prototype, carried out by locals, took almost 6000 hours (20% of total cost). About 90% of the materials (USD 35,600) were bought in the local market. Activities involved local unskilled labour at USD 5/day but also many hours of specialised technicians at USD 100/day.

The total investment cost of the prototype was about the same as (or less than) an equivalent industrial kiln dryer purchased with a furnace but without any energy system.

In Table 5 energy costs produced by different systems are compared considering component costs (Table 4), a life expectancy of 25 years and the cost of wood wastes feeding the furnace (USD 20/ton) or oil for diesel. For thermic energy, the furnace was the cheapest solution. The solar collector produces relatively cheap thermal energy. However, a plant with sufficient power requires a large surface (about 10 m² for 1 m³ of wood) and a large accumulation mass (about 0.5 m³ of water for 1 m³ of wood) corresponding to an investment of about USD 10,000 for 1 m³ of wood capacity.

Table 5. Comparison of energy costs.

	PV	SC	FR	DIESEL
USD/kWh	0.137	0.048	0.009	0.165

The photovoltaic plant requires the largest investment, but it generates electric energy without any other fuel cost. The only possible alternative in Yanonge would be electricity production by means of a diesel power unit. However, at the present rate of USD 0.16/kWh, such a unit costs about USD 25/m³ of dried wood for fuel alone and does not consider environmental costs from CO₂ emissions. In this context, the investments related to the photovoltaic plant are repaid after six years.

4. Conclusion

Based on available data, the prototype allows better drying than exterior conditions. In its actual size and configuration, it achieves a potential productivity target of about 20–30 m³/year of sawn board dried with a good quality of final MC (15%).

Making the chamber with local biomaterials resulted in an efficient, and sustainable solution, which is recyclable and biodegradable.

Thermal energy is the critical factor influencing the drying kinetic and cost of the plant. Regarding thermal energy, the furnace-burning biomasses turned out to be a good option, producing cheaper energy than any other solution. Nevertheless, it needs available biomass, as well as an operator to feed it and it generates CO₂ emissions and other pollutants. The use of solar collectors only instead of the furnace would require increasing its surface to at least 10 m² for each m³ of wood to reach the same energy power provided by the furnace and the same drying kinetic of DT2. This expansion should be accompanied by an equal expansion of the energy storage system using about 0.5 m³ of water for each m³ of wood for an optimal temperature management of the water. This solution would cost more but allow a zero emission process. Since solar collectors were efficient and made of simple technology, the prototype should focus next on providing locals with tools and skills to produce their own inexpensive solar collectors with a large extension, together with improved thermal insulation.

The electric energy for ventilation was the most expensive item, even if the free electricity allows investment in the photovoltaic plant to be repaid quickly. Additional investigations and trials should focus on further optimisation of ventilation energy needs. For example, low power electric vapour extractors and lower power internal fans could be integrated with a smart control algorithm to optimise its use as function of MC. It is also self-contained, which would allow a kiln to operate in a remote location without assistance.

The solar kiln prototype in Yanonge is at an early stage with significant potential for improvement. It is pointing the way toward substantial improvement of wood drying compared both to natural seasoning and traditional industrial drying with energy from fossil fuel. Beyond a positive impact on the local economy, the engagement of local people generated inclusion, participation and positive social dynamics. This can lay the foundation for a locally managed and sustainable activity.

Acknowledgements

Nardi International Italy and Livio Travan for the consultancy, adjustment support and supply of the actuators. Logica H&S Italy for the consultancy, adjustment support and supply of the electronic control. Andrea Melandri, I.T.T. 'G. Marconi', Padova (Italy) for the design of the section of the walls.

Disclosure statement

No potential conflict of interest was reported by the author(s).

Funding

This work was funded by European Union, grant number FED/2016/381-145 FORETS – Formation, Recherche, Environnement dans la Tshopo/Training, Research, Environment in the Tshopo and European Union, grant number ENV/2019/413-405 NPC – Nouveaux Paysages du Congo.

ORCID

Silvia Ferrari  <http://orcid.org/0009-0006-2816-7218>
 Ignazia Cuccui  <http://orcid.org/0000-0002-7385-4272>
 Paolo Cerutti  <http://orcid.org/0009-0003-3003-3516>
 Ottaviano Allegretti  <http://orcid.org/0000-0003-1772-2205>

References

- Allegretti, O., I. Cuccui, S. Ferrari, and A. Sione. 2009. "Dtouch-Drying has Never Been so Easy." In *The Future of Quality Control for Wood and Wood Products*, edited by D. J. Ridley-Ellis and J. R. Moore. Edinburgh: Edinburgh Napier University. Proceedings of the final conference of COST Action E53, pp. 30–38. ISBN 978-09566187-0-2
- Babiak, M. 2007. "Sorption Isotherms of Wood." In *Fundamentals of Wood Drying*, edited by P. Perré, 67–85. Nancy, France: A.R.B.O.LOR.
- Bekkioui, Naoual, Bilal Lamrani, Merlin Simo-Tagne, and Ndukwu Macmanus Chinenye. 2023. "Numerical Simulation and Experimental Validation of a Forced Convection Solar Dryer for North African Thuya Wood Stacks Under Meteorological Data of Essaouira City (Morocco)." *International Journal of Ambient Energy* 44 (1): 2296–2304. <https://doi.org/10.1080/01430750.2023.2234375>.
- Berinyuy, J. E., J. K. Tangka, and M. Weka Fotso. 2012. "Enhancing Natural Convection Solar Drying of High Moisture Vegetables with Heat Storage." *Agricultural Engineering International: CIGR Journal* 14:141–148.
- Bond, B. H., and O. Espinoza. 2016. "A Decade of Improved Lumber Drying Technology." *Current Forestry Reports* 2:106–118. <https://doi.org/10.1007/s40725-016-0034-z>.
- Boone, R. S., C. J. Kozlik, P. J. Bois, and E. M. Wengert. 1988. *Dry Kiln Schedules for Commercial Woods – Temperate and Tropical 1988, Gen. Tech. Rep. FPL-GTR-57*, pp. 158. Madison, WI: U.S. Department of Agriculture, Forest Service, Forest Products Laboratory.
- Bracamonte, J., J. Parada, J. Dimas, and M. Baritto. 2015. "Effect of the Collector Tilt Angle on Thermal Efficiency and Stratification of Passive Water in Glass Evacuated Tube Solar Water Heater." *Applied Energy* 155:648–659. <https://doi.org/10.1016/j.apenergy.2015.06.008>.
- Cascone, S., R. Rapisarda, and D. Cascone. 2019. "Physical Properties of Straw Bales as a Construction Material: A Review." *Sustainability* 11 (12): 3388. <https://doi.org/10.3390/su11123388>.
- Chauhan, Yagnesh B., and Pravin P. Rathod. 2020. "A Comprehensive Review of the Solar Dryer." *International Journal of Ambient Energy* 41:348–367. <https://doi.org/10.1080/01430750.2018.1456960>.
- CITES (Convention on International Trade in Endangered Species of Wild Fauna and Flora). 2023. Appendices I, II & III (21/05/2023) p. 71. <https://cites.org/sites/default/files/eng/app/2023/E-Appendices-2023-05-21.pdf>.
- Duhesme, C., M. Gally, S. Glannaz, C. Hervo, Y. Kone, G. Lescuyer, L. Mbonayem, P. Nakoe, A. Ngoya Kessy, P. Lahann, et al. 2022. "The Evolution of the Wood Subsector in the Congo Basin." In *The Forests of the Congo Basin: State of the Forests 2021*, edited by R. Eba'a Atyi, F. Hiol Hiol, G. Lescuyer, P. Mayaux, P. Defourny, N. Bayol, F. Saracco, D. Pokem, R. Sufo Kankeu, and R. Nasi, 53–54. Bogor: CIFOR.
- EDG (European Drying Group) – Recommendation. 1994. *Assessment of Drying Quality of Timber*. Pilot edition. Ed. J. Welling. [http://www.timberdry.net/downloads/EDG/EDG-Recommendation\(eng\).pdf](http://www.timberdry.net/downloads/EDG/EDG-Recommendation(eng).pdf).
- Elustondo, D., N. Matan, T. Langrish, and S. Pang. 2023. "Advances in Wood Drying Research and Development." *Drying Technology* 41 (6): 890–914. <https://doi.org/10.1080/07373937.2023.2205530>.
- European Standard 14298: 2018 Saw Timber – Assessment of Drying Quality. 2018.
- Gnansounou, E., C. M. Alves, and J. K. Raman. 2017. "Multiple Application of Vetiver Grass – a Review." *International Journal of Environmental Science* 2:125–141.
- Guizol, P., L. Mbonayem, A. Awono, D. Djossi, P. Tabi, M. A. Ngobieng, B. P. Ntirumenyerwa Mihigo, P. Lungungu, R. Mbuyu Kimpesa Kasulo, C. Ndikumagenge, et al. 2022. "Land Use Planning and Impacts on the Sustainable Management of Forest Ecosystems in Central Africa." In *The Forests of the Congo Basin: State of the Forests 2021*, edited by R. Eba'a Atyi, F. Hiol Hiol, G. Lescuyer, P. Mayaux, P. Defourny, N. Bayol, F. Saracco, D. Pokem, R. Sufo Kankeu, and R. Nasi, 291–294. Bogor: CIFOR. <https://doi.org/10.17528/cifor/008700>.
- Hengsadeekul, T., and P. Nimityongskul. 2004. "Construction of Paddy Storage Silo Using Vetiver Grass and Clay." *Assumption University Journal of Technology* 7 (3): 120–128.
- Joly, P., and F. More-Chevalier. 1980. *Théorie, Pratique & Économie du Séchage des bois*, edited by H. Vial, Dourdan, pp. 21–49.
- Lamrani, B., N. Bekkioui, M. Simo-Tagne, and M. C. Ndukwu. 2022. "Recent Progress in Solar Wood Drying: An Updated Review." *Drying Technology* 41 (5): 605–627. <https://doi.org/10.1080/07373937.2022.2112048>.
- Lescuyer, G., P. O. Cerutti, P. Tshimpanga, F. Biloko, B. Adebun-Abdala, R. Tsanga, R. I. Yembe-Yembe, and E. Essiane-Mendoula. 2014. *Le marché domestique du sciage artisanal en République Démocratique du Congo : État des lieux, opportunités, défis 2014. Document occasionnel 110*. Bogor: CIFOR.
- Logica H&S SRL Electronics for Wood Processing. 2023. Accessed October 2023. www.logica-hs.it/en/dtouch.
- López-Sosa, L. B., J. Nunez-González, A. Beltrán, M. Morales-Máximo, M. Morales-Sánchez, M. Serrano-Medrano, and C. A. García. 2019. "A new Methodology for the Development of Appropriate Technology: A Case Study for the Development of a Wood Solar Dryer." *Sustainability* 11:5620. <https://doi.org/10.3390/su11205620>.
- Mathew, Adarsh Abi, and T. Venugopal. 2021. "Solar Power Drying System: A Comprehensive Assessment on Types, Trends, Performance and Economic Evaluation." *International Journal of Ambient Energy* 42 (1): 96–119. <https://doi.org/10.1080/01430750.2018.1507933>.
- Ndukwu, M. C., L. Bennamoun, and F. I. Abam. 2018. "Experience of Solar Drying in Africa: Presentation of Design, Operations, and Models." *Food Engineering Reviews* 10:211–244. <https://doi.org/10.1007/s12393-018-9181-2>.
- Nimityongskul, P., S. Panichnava, and T. Hengsadeekul. 2003. "Use of Vetiver Grass ash as Cement Replacement Materials" Proceedings of The Third International Conference on Vetiver (ICV-3), Guangzhou, China, 6–9 October.
- Pratt, G. H. 1974. *Timber Drying Manual, Building Research Establishment, Department of the Environment*. London: HMSO.
- Simo-Tagne, M., and L. Bennamoun. 2018. "Numerical Study of Timber Solar Drying with Application to Different Geographical and Climatic Conditions in Central Africa." *Solar Energy* 170:454–469. <https://doi.org/10.1016/j.solener.2018.05.070>.
- Solargis. 2023. Accessed November 6, 2023. <http://solargis.com/maps-and-gis-data/overview>.
- TROPIC 7 The Main Technological Characteristics of 245 Tropical Wood Species. 2017. CIRAD's Biomass, Wood, Energy, Bioproducts Research Unit (BioWooEB). <https://doi.org/10.18167/74726F706978>.
- Udomkun, P., S. Romuli, S. Schock, B. Mahayothee, M. Sartos, T. Wossen, E. Njukwe, B. Vanlauwe, and J. Müller. 2020. "Review of Solar Dryers for Agricultural Products in Asia and Africa: An Innovation Landscape Approach." *Journal of Environmental Management* 268:110730. <https://doi.org/10.1016/j.jenvman.2020.110730>.